INVESTIGATING THE EFFECT OF A TARGET'S TIME-VARYING AXIS OF ROTATION ON ISAR IMAGE DISTORTION

M.Y. Abdul Gaffar*, W. Nel*

*Council for Scientific and Industrial Research (CSIR), South Africa, <ynagaffar@csir.co.za>, <wajnel@csir.co.za>

Keywords: ISAR imaging, image distortion, 3-D motion, quaternions

Abstract

This paper investigates the effect of a target's time-varying axis of rotation on ISAR image distortion. ISAR has potential in assisting with the classification of non-cooperative targets. However, a blurred ISAR image is not desired as this may lead to misleading classification results. Research has been done to understand some of the causes of distortion in ISAR under the limited assumptions that the target's motion is confined to a 2D plane over the CPI. In this paper, more realistic 3D target motion is considered where the target's axis of rotation is varied over the CPI. Measured motion data of a sailing yacht at sea is used to investigate the complex effects caused by a target's changing axis of rotation and its effect on ISAR blurring. Future research is required to find ways of handling such complex motion in a robust manner.

1 Introduction

Inverse Synthetic Aperture Radar (ISAR) is a radar imaging technique that is used to estimate the position, amplitude and phase of scattering centers of a target. Typical targets of interest to both the civilian and military communities include aircraft and ships. ISAR imagery has potential of exhibiting important discriminative information that can be used to perform Non-cooperative Target Recognition (NCTR).

Unfortunately (unlike SAR), ISAR imaging relies on the target's own motion that is typically non-cooperative and often complex in nature such as the motion of a sailing yacht in rough sea conditions. This chaotic motion may lead to significant distortion in the resulting 2D ISAR image of the target using conventional algorithms [1, 2]. Much research has focused on the effect of the target's rotation motion on the distortion of the resulting ISAR image [4-7]. However, most of these results assume that the rotational motion of the target is confined to a 2D plane that is orthogonal to the radar-target line of sight during the Coherent Processing Interval (CPI) [8]. Some work has also be done in using the complex motion to form 3D ISAR imagery [3]. Some mathematical analysis has been done to better understand the causes of distortion in ISAR [4]. Apart form motion, other causes such as non point-scatterer like scattering mechanisms could also cause image blurring.

For NCTR, an unfocused ISAR image can lead to incorrect classification. Motion induced factors that influences distortion includes the target's axis of rotation and the rotation rate [8]. It is well known that a uniformly rotating target can induce a time-varying Doppler frequency over a large CPI [5], which causes scatterer migration through range-doppler cells. ISAR distortion due to non-linear rotation motion was investigated in [6]. To the authors' knowledge, existing literature does not adequately address the influence of a target's axis of rotation on ISAR image distortion.

To this end, this work investigates the effect of a time-varying axis of rotation on ISAR image distortion. A novel approach (to ISAR literature) of using quaternions to represent the target's rotation is pursued, since it elegantly expresses the axis of rotation. The approach makes intuitive sense here, since the component of the axis of rotation that is orthogonal to the radar-target line of sight, corresponds to the image projection plane, and the rate of target rotation determines the scaling factor for the cross range component of the imaging plane. As the projected axis of rotation changes in the plane that is orthogonal to the radar-target line of sight, it has the effect of changing the image projection plane which gives rise to blurring effects.

2 Mathematical model of a target with 3D rotation motion

The rotation of the target and transformations between two co-ordinate systems can be expressed using quaternion algebra.

2.1 The quaternion as a rotational operator

The concept of quaternions was introduced by Hamilton as an extension of complex numbers [9, 10]:

$$q = \begin{bmatrix} q(1) & q(2) & q(3) & q(4) \end{bmatrix}^T = \begin{bmatrix} s & \mathbf{v} \end{bmatrix}^T \qquad (1)$$

where $s \in \Re$ and $\mathbf{v} \in \Re^3$ are the complex vector and real scalar parts of the quaternion respectively.

A point in 3-D space, $\mathbf{p} = \begin{bmatrix} x & y & z \end{bmatrix}$ can be transformed into a 4-D vector quaternion $p = \begin{bmatrix} 0 & \mathbf{p} \end{bmatrix}^T$. If $\mathbf{h} = \begin{bmatrix} h_1 & h_2 & h_3 \end{bmatrix}$

represents a normalised axis of rotation that passes through the origin and θ represents the angle of rotation, then the unit quaternion representing the rotation can be written as:

$$q = \left[\cos(\theta/2) \quad \mathbf{h}\sin(\theta/2)\right]^T \tag{2}$$

Let $\mathbf{a} = \left[a_x \;\; a_y \;\; a_z\right]$ and $\mathbf{b} = \left[b_x \;\; b_y \;\; b_z\right]$ represent two points in 3D space. The quaternion rotational operator that rotates the point $\mathbf{a}$ counter-clockwise through an angle θ onto $\mathbf{b}$ is given by:

$$b = q \otimes a \otimes q^* \tag{3}$$

where $\otimes$ denotes quaternion multiplication and a, b are quaternion vectors of the 3-D vectors $\mathbf{a}$ and $\mathbf{b}$. Note that the rotated point $\mathbf{b}$ in 3D is given by the vector component of the quaternion b.

2.2 Transformation from the local to the global co-ordinate frame

In this investigation we consider a sea vessel with only rotation motion and assume that any translation motion has been compensated. In Figure 1, there are two co-ordinates axes. The radar's co-ordinate axes (U,V,W) form the global non time-varying co-ordinate axes. On the contrary, the target's local co-ordinate axes (X_n, Y_n, Z_n) rotates when the target experiences 3D rotational motion, and is considered time-varying. In Figure 1, $R_k(n)$ denotes the distance from the radar to the target's k^{th} scatterer for time t_n and R_0 represents the distance from the radar to the target's center of rotation. In this section we aim to express the co-ordinates of the target's k^{th} scatterer in the radar's co-ordinate axes as the target rotates over the CPI.

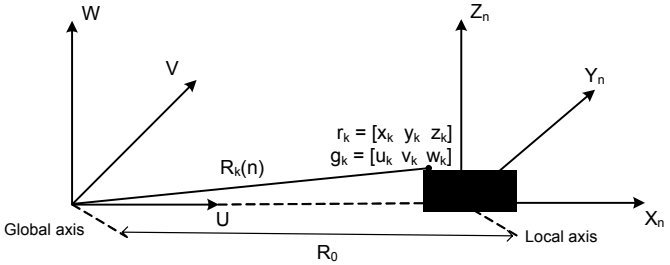

Figure 1: System model of the radar and the target showing the global and the local co-ordinates axes

During the time interval $\Delta t_n = t_n - t_{n-1}$, the target's local co-ordinate axes rotates from $(X_{n-1}, Y_{n-1}, Z_{n-1})$ to (X_n, Y_n, Z_n) as seen by the global co-ordinate system, where n refers to the target's discretised rotation over the CPI. We express the co-ordinates of the k^{th} scatterer in the local $\mathbf{r}_k$ and global $\mathbf{g}_k$ co-ordinate system as:

$$\mathbf{r}_k = \left[x_k \;\; y_k \;\; z_k\right] \tag{4}$$

$$\mathbf{g}_k = \left[u_k \;\; v_k \;\; w_k\right] \tag{5}$$

Assume that the start time for the CPI is denoted as t_0. Then at t_1, the target has undergone one step of discrete rotation. The projection of the k^{th} scatterer's local co-ordinates $\mathbf{r}_k$ onto the radar's global co-ordinate axes can be expressed as:

$$g_{k,1} = q_{s,1}\left(q_{s,0} r_k \left(q_{s,0}\right)^*\right)\left(q_{s,1}\right)^* \tag{6}$$

where $q_{s,0}$ is the quaternion that represents the initial orientation of the target with respect to the global axes, $q_{s,1}$ denotes the target's rotation over Δt_1 and $g_{k,1}$ denotes the quaternion vector $g_{k,1} = \left[0 \;\; \mathbf{g}_{k,1}\right]$, $\mathbf{g}_{k,1} = \left[u_{k,1} \;\; v_{k,1} \;\; w_{k,1}\right]$ for time t_1. The expression $g_{k,0} = q_{s,0} r_k \left(q_{s,0}\right)^*$ would correspond to the initial global co-ordinates of the scatterer.

After N discrete rotations, the global co-ordinates of k^{th} scatterer at time instant t_N can be expressed as:

$$g_{k,N} = q_{s,N} \cdots \left(q_{s,1}\left(q_{s,0} r_k \left(q_{s,0}\right)^*\right)\left(q_{s,1}\right)^*\right) \cdots \left(q_{s,N}\right)^* \tag{7}$$

3 Simulation of three cases in point

We investigate three cases of motion induced Doppler frequency due to a time varying axis of rotation over the CPI. Case 1 deals with a simulated time-varying axis of rotation with constant angular rotation rates. Cases 2 and 3 deals with more realistic rotation based on measured data from an instrumented sailing yacht.

3.1 Case 1: Simulated time-varying axis of rotation

Assume that the target's axis of rotation rotates due to an unwanted perturbation about a fixed axis $\mathbf{h}_m = \left[h_{m,1} \;\; h_{m,2} \;\; h_{m,3}\right]$ that is aligned with the radar Line Of Sight (LOS). The fixed axis rotates at a constant rate of Ω_m (see Figure 2). The rotation angle θ_m for one discrete rotation can be expressed as:

$$\theta_m = \Omega_m \Delta t \tag{8}$$

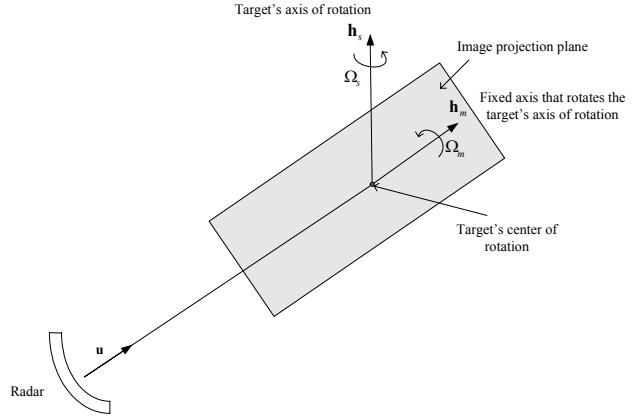

Figure 2: Target's time-varying axis of rotation over the CPI

The target also rotates with a constant rotation rate of Ω_s about an axis of rotation $\mathbf{h}_{s,n} = \begin{bmatrix} h_{s1,n} & h_{s2,n} & h_{s3,n} \end{bmatrix}$ for the n[th] discrete rotation[1]. The quaternion representing the rotation of the target for time t_n is given by:

$$q_{s,n} = q_{m,n} q_{s,n-1} \left(q_{m,n}\right)^* \tag{9}$$

where $q_{m,n}$ represents the rotation about the fixed axis $\mathbf{h}_m$ through a angle of θ_m and $q_{s,n}$ represents the rotation about the target's axis of rotation $\mathbf{h}_{s,n}$ through an angle θ_s. The transformation of the k^{th} scatterer's co-ordinates from the local axes to the global axes is given by (7).

3.2 Case 2: Fixed rate rotation with realistic perturbation

For this case, we consider a point scatterer simulation of a sailing yacht (see Appendix A) with the aim of generating a side-view ISAR image. At the start of the CPI, the simulated target is sailing towards the radar with an initial aspect of 20°. Through the CPI the target undergoes an unrealistically sustained constant pitch rate, zero roll rate and it is being perturbed by a time-varying yaw rate based on real data from an instrumented measurement of a yacht[2]. Figure 5 (a) and (b) details the roll, pitch and yaw motion used in the simulation.

3.3 Case 3: Real complex 3D motion data

The third case considered in simulation of the yacht is where the point scatterer model experiences motion based completely on real data as shown in Figure 7 (a) and (b). The target model has an initial aspect of approximately 20 deg relative to the radar (nose-on view).

The motion data was recorded in Euler angles using the Aerospace sequence of roll ϕ, pitch ψ and yaw α.

3.4 Motion induced doppler frequency

As the target experiences complex 3D motion, the distance from the radar to the target's k^{th} scatterer changes. This leads to a motion induced Doppler frequency. In this section, we express the motion induced Doppler frequency of the k^{th} scatterer over the CPI.

We assume that the radar continuously tracks the target in such a way that the global U axis is always aligned to the target's center of rotation (see Figure 1). The range from the radar to the k^{th} scatterer of the target at time t_n can be expressed as:

$$R_k(n) = \sqrt{\left(u_{k,n}\right)^2 + \left(v_{k,n}\right)^2 + \left(w_{k,n}\right)^2} \tag{10}$$

R_0 is the distance between the radar and the target's center of rotation and $R_k(n)$ denotes the range from the radar to the k^{th} scatterer for time t_n.

The motion induced Doppler frequency in the continuous time domain can be expressed as:

$$f_D(t) = \frac{2f}{c}\frac{dR(t)}{dt} \tag{11}$$

or in discrete form as:

$$f_D(n) = \frac{2f}{c}\left[\frac{R(n) - R(n-1)}{\Delta t}\right] \tag{12}$$

where Δt is the time period between two discrete rotations

4 Simulation results

Table 1 summarises the simulation parameters that were used for ***case 1***. The CPI was chosen to be 1s which corresponds to a Doppler resolution of 1Hz. All positive rotations are defined as a clockwise rotation in a right handed co-ordinate system.

Table 1: Simulation parameter values

Parameter description	*Symbol*	*Value*
k^{th} scatterer local co-ordinates	$\mathbf{r}_k$	$\begin{bmatrix}10 & 0 & 5\end{bmatrix}$
Target's axis of rotation	$\mathbf{h}_{s,0}$	$\begin{bmatrix}0 & 0 & 1\end{bmatrix}$
Target's rotation rate	Ω_s	2°/s
Fixed axis	$\mathbf{h}_m$	$\begin{bmatrix}1 & 0 & 0\end{bmatrix}$
Fixed axis's rotation rate	Ω_m	$\{0,2,4,6,8\}$ °/s
Time period between two discrete rotations	Δt	0.01s

For the rates of rotation as specified in Table 1, the effect on the scatterer instantaneous Doppler frequency can be seen in curves (b)-(e) of Figure 3. The Doppler spread[3] is greater than the Doppler resolution of 1 Hz. This will cause the scatterer to experience migration through range-doppler cells, leading to blurring in the resultant ISAR image as shown in [4].

To avoid blurring, one could choose to process the image as an unfocused ISAR image so that the rotation angle and the rotation of the target's axis are such that the change in the Doppler spectrum is much less than the Doppler resolution. It is believed that a polar reformatting type algorithm for ISAR [11] would not be suited to solve the blurring problem since such algorithms assume that the target's axis of rotation is fixed over the CPI.

[1] This case corresponds to a standard *top-view* ISAR imaging scenario with a perturbation causing the axis of rotation to rotate linearly in the plane orthogonal to the radar-target LOS over the CPI.

[2] The data for case 2 and 3 are based on measurements of the attitude and position of an instrumented yacht during an ISAR imaging campaign in Simonstown, South Africa in June 2007. Actual ISAR imaging results were not yet available at the time of paper submission.

[3] Where Doppler spread is defined as the maximum difference in Doppler over the CPI.

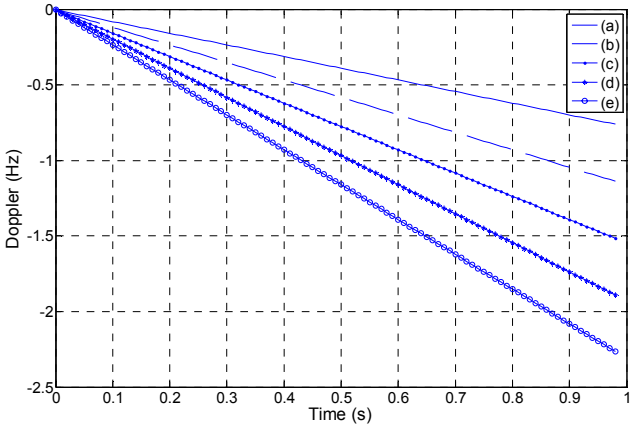

Figure 3: Motion induced Doppler spectrum of the k^{th} scatterer $\mathbf{r}_k = [10\ \ 0\ \ 5]^T$ for $\Omega_s = 2°/\text{s}$ and Ω_m equal to (a) $0°/\text{s}$, (b) $2°/\text{s}$, (c) $4°/\text{s}$, (d) $6°/\text{s}$ and (e) $8°/\text{s}$.

Figure 4 shows the effect of ISAR distortion for a simple test target corresponding to case 1. The test target is made of three scatterers: $\mathbf{r}_A = [0\ \ 0\ \ 0]$, $\mathbf{r}_B = [-8\ \ 0\ \ 0]$ and $\mathbf{r}_C = [10\ \ 0\ \ 8]$. The fixed axis's rotation rate is $\Omega_m = 10°/s$ and the other simulation parameter values are the same as Table 1. Scatterer $\mathbf{r}_A$ corresponds to the target's center of rotation. Since it does not experience cell migration, it is well-focused in the ISAR image. Scatterer $\mathbf{r}_B$ lies in the image projection plane and its change in Doppler is less than the Doppler resolution over the CPI. It corresponds to a scatterer of an unfocused ISAR image. Scatterer $\mathbf{r}_C$ on the other hand experiences cell migration over the CPI, and this causes blurring in the resulting ISAR image.

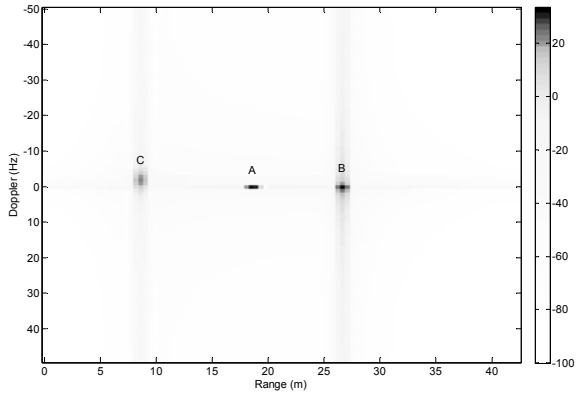

Figure 4: ISAR image (unfocused) of three scatterers for $\Omega_s = 2°/\text{s}$ and Ω_m equal to 10°/s.

Figure 5 (c) and (d) shows the unfocused ISAR images (i.e. no polar-reformatting) for the trivial case of a fixed axis of rotation and the rotation of the axis of rotation as described in ***case 2*** respectively[4]. It is clear that the additional yaw rate component contributes to a large amount of defocus in the image. To analyse this result, a plot was made of the instantaneous Doppler of each of the scatterers in the simulation model, shown in Figure 5 (e) and (f). Although the heading rates and absolute heading deviation is minimal, the final change in Doppler frequency due to the additional component of rotation is significant, and the image will clearly show tremendous defocus. It is instructive to note that the total Doppler bandwidth of the target is still within the same limits. Also, the simulation was set up such that the total effective aspect change of the target over the CPI was approximately 1° in both cases.

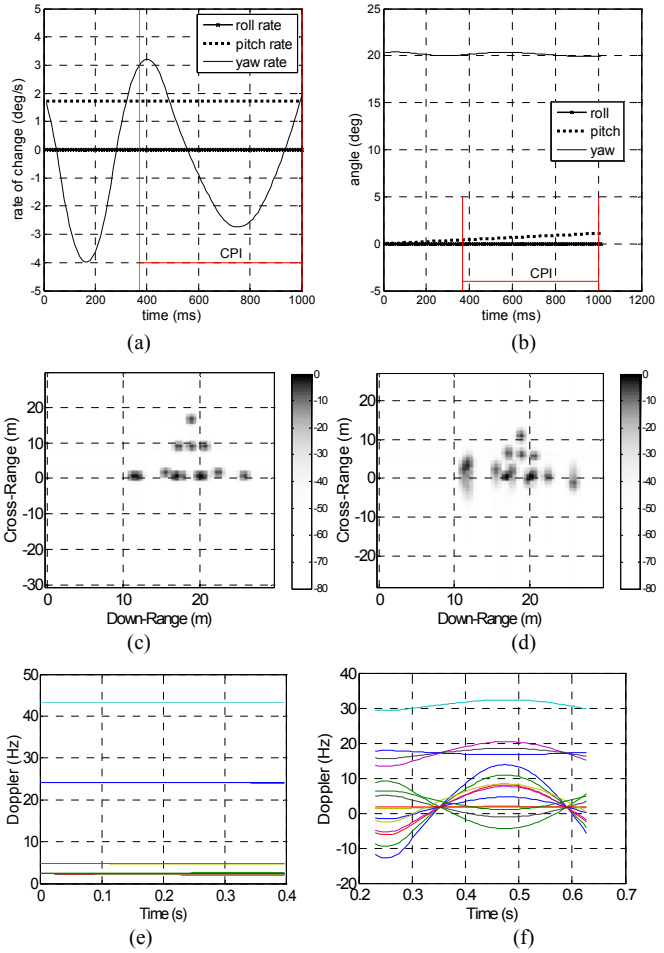

Figure 5: Rotation rates (a), and values (b) for the target in case 2, comparing an ISAR image with a fixed pitch axis of rotation (c) with an ISAR image of the yacht possessing case 2 motion (d), and their corresponding instantaneous Doppler per scatterer shown in (e) and (f) respectively.

Figure 6 shows the angle of the effective axis of rotation relative to the radar's V axis in a plane orthogonal to U as defined in Figure 1. It is clear that the additional yaw rate, results in significant changes in the effective Doppler generating axis of rotation. This gives rise to significant blurring effects. Note also the high degree of correlation between the Doppler of the blurred scatterers and the angle of the effective axis of rotation.

Figure 7 (a) and (b) shows a summary of the results for ***case 3***, where the target now experiences complete 3D motion. The resultant ISAR image shows completely

[4] The ISAR images are shown in dB relative to peak power.

unacceptable blur, which most likely cannot be compensated by standard autofocus and polar reformatting techniques due to the many effective projection and scale changes observed during the CPI by the varying time axis and varying rate of rotation.

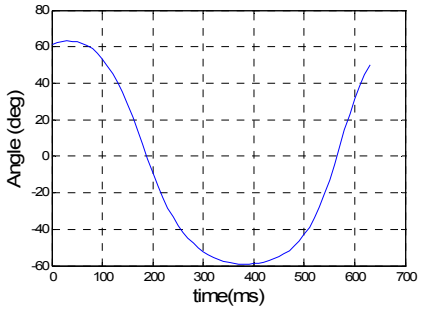

Figure 6: Resultant change in angle of the effective axis of rotation in the plane orthogonal to the radar-target LOS over the CPI for ***case 2***.

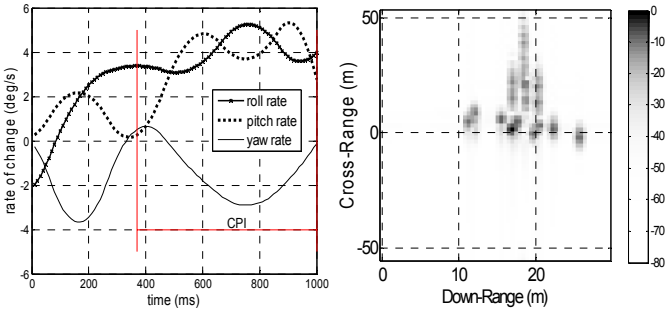

Figure 7: Rotation rates (a) and ISAR image (b) for ***case 3***.

5 Conclusions

This paper examined the effect of a target's time-varying axis of rotation on ISAR distortion. The rotation motion of the target was mathematically represented using quaternions which made it easy to manipulate the angle and axis of rotation. Different types of motion ranging from trivial single axis rotation to complex 3D target motion were analysed. The effect of a time varying axis of rotation on the rotation-motion induced a Doppler spectrum was shown. Simulation results show that ISAR blurring is sensitive to a target's time-varying axis of rotation over the CPI. In order to achieve consistent ISAR results, the influence of both the rotation rate and target's time-varying axis of rotation on the motion induced Doppler spectrum needs to be considered in future research.

Acknowledgements

This work was supported by Armscor and the South African Department of Science and Technology. Sincere thanks to Dr R.T. Lord, Mr F. Anderson, and Mr A. le Roux for fruitful comments and suggestions.

References

[1] C. C. Chen, H. C. Andrews, "Target-Motion-Induced Radar Imaging", *IEEE Transactions on Aerospace Systems*, **1**, pp. 2-14, (1980).

[2] B. Haywood, R.J. Evans, "Motion Compensation for ISAR Imaging", *Proceedings of Australian Symposium on Signal Processing and Applications*, pp. 112-117, (1989).

[3] R. T. Lord, W. Nel, M. Y. Abdul Gaffar, "Investigation of 3-D RCS Image Formation of Ships Using ISAR", *Proc. European Conference on Synthetic Aperture Radar*, EUSAR 2006, Dresden, Germany, May 2006.

[4] V. C. Chen, W. J. Miceli, "Time-varying spectral analysis for radar imaging of maneuvering targets", *IEE Proceedings of Radar, Sonar and Navigation*, 145, pp. 262-268, (1998).

[5] D. R. Wehner, 'High-Resolution Radar', Second Edition, Norwood, MA, Artech House, (1995).

[6] S. K. Wong, G. Duff, E. Riseborough, "ISAR Image Distortion due to Small Perturbed Motion and Restoration of Distorted Images by Time-Frequency Analysis", *Proceedings of SPIE*, **5102**, Florida, USA, April 22-25, pp. 200-212, (2003).

[7] V. C. Chen, R. Lipps, "ISAR imaging of small craft with roll, pitch and yaw analysis', *Proc. IEEE International Radar Conference*, Verona, NY, pp. 493-498, (2000).

[8] T. Sparr, "ISAR – Radar imaging of targets with complicated motion" *Proc. IEEE International Conference on Image Processing (ICIP)*, Singapore, pp. 5-8, (2004).

[9] W. R. Hamilton, "Elements of Quaternions", *London: Longmar and Co.,* (1866).

[10] J. B. Kuipers, "Quaternions and Rotation Sequences", *Princeton University Press,* (1999).

[11] R. Lipps, D. Kerr, "Polar reformatting for ISAR imaging", *Proc. IEEE National Radar Conference*, Texas, Dallas, pp. 275-280, (1998).

Appendix A – Simple scatterer model of yacht

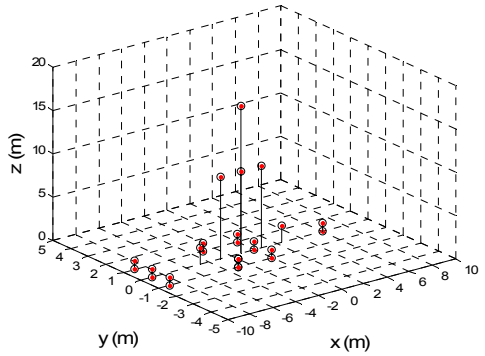

Figure A1: Simple point scatterer model of a yacht. The mast height is 17m and the target width and length is 2m and 15m respectively